
LATTICE DYNAMICS
AND PHASE TRANSITIONS

Metal–Dielectric Transitions, Magnetism, and Electronic Structure in a System of Manganese-Doped Vanadium Sulfides

G. V. Loseva, S. G. Ovchinnikov, A. D. Balaev, and N. I. Kiselev

Kirenskiĭ Institute of Physics, Siberian Division, Russian Academy of Sciences, Akademgorodok, Krasnoyarsk, 660036 Russia
e-mail: sgo@post.krascience.rssi.ru

Received in final form, September 17, 1999

Abstract—The effect of the manganese doping of vanadium monosulfide in a system of the $V_{1-x}Mn_xS$ ($0 < x \leq 0.3$) solid solutions on their structure and thermal, electrical, and magnetic properties has been investigated. The metal–dielectric transitions are revealed in the studied ranges of concentrations and temperatures. These transitions are accompanied by a change in the magnetic properties. It is demonstrated that the correlation in changes of the electrical and magnetic properties of the sulfides under investigation is characteristic of the metal–dielectric transitions in strongly correlated systems. © 2000 MAIK “Nauka/Interperiodica”.

Recently, considerable interest has been expressed by researchers in physical properties of doped vanadium sulfide systems with a metal–dielectric transition, for example, $La_{1-y}R_yS_{1+a}VS_2$ ($R = Sr$ or Rb) [1], $La_{1.17-x}Sr_xVS_{3.17}$ [2], and $BaVS_3$ [3]. In similar systems, strong electron correlations play a significant part in the formation of spin states and realization of complex mechanisms responsible for the metal–dielectric transitions. Moreover, it has been found that, at a certain concentration of impurities, the copper-free sulfide systems exhibit a state of an “anomalous metallic phase,” whose physical properties are similar to the properties of superconducting oxide cuprates [4].

In this respect, the study of the electrical and magnetic properties of doped vanadium sulfide systems based on vanadium monosulfide [5] has been an urgent problem.

The present paper reports the results of our investigation concerned with the influence of the cationic replacement of a vanadium ion by a manganese ion in vanadium monosulfide on the structure and thermal, electrical, and magnetic properties of the $V_{1-x}Mn_xS$ ($0 < x \leq 0.3$) system at different compositions, temperatures, and magnetic fields.

The mechanisms of the metal–dielectric transitions, specific features of electronic and magnetic states of sulfides in the system under consideration are analyzed taking into account strong electron correlations. A scheme of the electronic structure of the $V_{1-x}Mn_xS$ system is considered.

1. EXPERIMENTAL TECHNIQUE

Polycrystalline samples of the $V_{1-x}Mn_xS$ system with compositions in the range $0 < x \leq 0.4$ were prepared from the pure elements by the replacement of vanadium by manganese in the VS compound in evacuated silica tubes upon heat treatment at a temperature of 1000 K for four days.

uated silica tubes upon heat treatment at a temperature of 1000 K for four days.

X-ray diffraction analysis of the samples was carried out on a DRON-3M diffractometer (CuK_α radiation) at a temperature of 300 K. The curves of differential thermal analysis (DTA) were obtained on a MOM derivatograph in evacuated silica tubes of special form at a rate of 10 K/min in the temperature range 300–1300 K upon heating and cooling.

The low-temperature measurements of the heat capacity C_p were performed with a differential scanning calorimeter in the range 100–300 K at rates of 8 and 16 K/min.

The electrical resistivity was measured by the dc potentiometer method in the temperature range 80–300 K on samples in the form of parallelepipeds $10 \times 5 \times 3$ mm in size. The samples were preliminarily annealed in evacuated silica tubes at 1300 K.

The magnetization of the $V_{1-x}Mn_xS$ sulfides was measured on an automated vibrating magnetometer with a superconducting solenoid [6] in the temperature range 4.2–300 K in magnetic fields of 0.5–50.0 kOe by using the same samples as in the measurements of the electrical resistivity. The temperature dependences of the magnetization were obtained upon heating the samples.

2. RESULTS

2.1. Concentration dependences of the electrical and magnetic properties of the $V_{1-x}Mn_xS$ solid solutions. According to the data of X-ray diffraction analysis, all the solid solutions studied have a superstructure of the distorted low-temperature β -VS phase (B31, MnP-type). The results of X-ray structure analysis are confirmed by the data obtained.

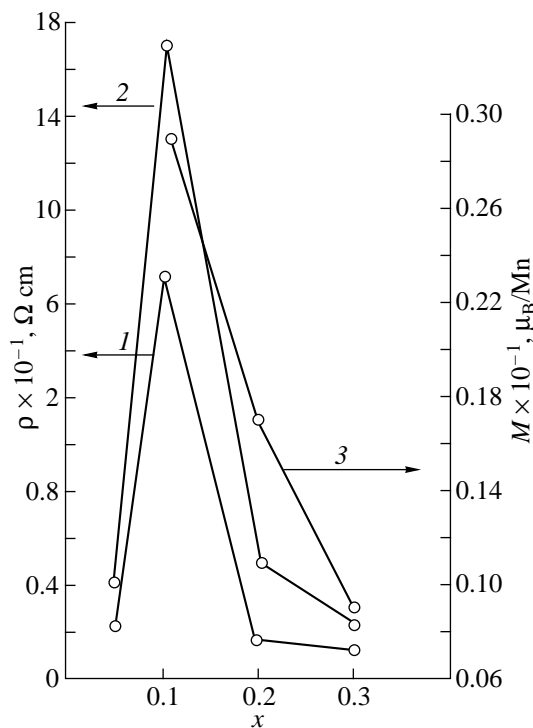


Fig. 1. Concentration dependences of the electrical resistivity ρ at temperatures of (1) 300 and (2) 80 K and (3) concentration dependence of the magnetic moment M per the Mn atom (μ_B/Mn) in a magnetic field of 2 kOe at $T = 80$ K in the $\text{V}_{1-x}\text{Mn}_x\text{S}$ system ($0.05 \leq x \leq 0.3$).

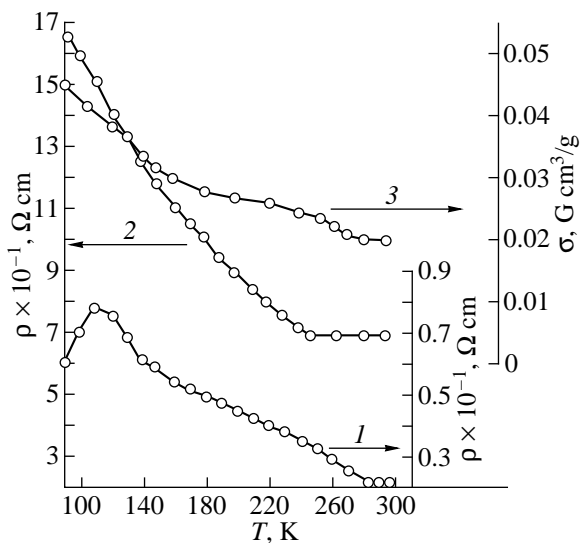


Fig. 2. Temperature dependences of the electrical resistivity in the $\text{V}_{1-x}\text{Mn}_x\text{S}$ system with compositions (1) $x = 0.05$ and (2) $x = 0.1$ and (3) temperature dependence of the magnetization σ at $x = 0.1$ in a magnetic field of 2 kOe in the range 80–300 K.

The high-temperature reversible endothermal effects in the range 800–900 K, which are characteristic of the metal–dielectric transitions in the VS monosulfide (the electron transition is observed at the tempera-

ture $T_c \sim 900$ K, and the structural transition proceeds at $T_S \sim 800$ K [5]), are also revealed in all the $\text{V}_{1-x}\text{Mn}_x\text{S}$ sulfides under investigation.

Figure 1 displays the concentration dependences of the electrical resistivity ρ of the $\text{V}_{1-x}\text{Mn}_x\text{S}$ solid solutions with compositions in the range $0.05 \leq x \leq 0.3$ at temperatures $T = 300$ (curve 1) and $T = 80$ K (curve 2). As is seen from Fig. 1, the maximum electrical resistivity is observed in the samples at $x = 0.1$ ($\rho_{80\text{ K}} = 17.2 \times 10^{-1} \Omega \text{ cm}$, $\rho_{300\text{ K}} = 7.1 \times 10^{-1} \Omega \text{ cm}$); their conductivity is three orders of magnitude smaller than the conductivity of the VS monosulfide ($\rho_{80\text{ K}} = 0.65 \times 10^{-3} \Omega \text{ cm}$). In the samples with $x = 0.3$, the ρ value decreases by three orders of magnitude at 80 K and by two orders of magnitude at 300 K.

The concentration dependence of the magnetic moment M per the Mn atom (μ_B/Mn) (in terms of Bohr's magneton) for the $\text{V}_{1-x}\text{Mn}_x\text{S}$ ($0.1 \leq x \leq 0.3$) system at temperature $T = 80$ K is also shown in Fig. 1 (curve 3). Similar concentration dependences $\rho(x)$ and $M(x)$ are found in the $\text{Fe}_x\text{V}_{1-x}\text{S}$ system [7].

2.2. Temperature dependences of the electrical and magnetic properties of the $\text{V}_{1-x}\text{Mn}_x\text{S}$ solid solutions.

Figure 2 depicts the temperature dependences $\rho(T)$ for the $\text{V}_{1-x}\text{Mn}_x\text{S}$ samples with compositions $x = 0.05$ (curve 1) and $x = 0.1$ (curve 2) upon cooling in the range from 300 to 80 K. As can be seen from Fig. 2, the temperature dependence of the electrical resistivity of the sample with $x = 0.05$ is typical of semimetals in the range 80–110 K and exhibits activation behavior in the range 110–280 K. The composition with $x = 0.1$ is characterized by a conductivity of the activation type in the range 80–240 K. It should be noted that, in the given temperature range, the compositions with $x = 0.0, 0.02$, and 0.05 show no anomalies in the heat capacity C_p . At the same time, the composition with $x = 0.1$ displays a very weak anomaly in C_p at $T = 205$ K.

In the temperature range 240–260 K (curve 2 in Fig. 2), the conductivity of the activation type for the sample with $x = 0.1$ changes to the semimetallic conductivity, which is accompanied by the appearance of a knee in the temperature dependence of the magnetization $\sigma(T)$ at $T = 250$ K (curve 3 in Fig. 2).

An abrupt increase in the electrical resistivity ρ (by three orders of magnitude) for the samples with $x = 0.1$ (Figs. 1, 2) suggests that, at $x_c = 0.1$, the concentration metal–dielectric transition takes place. This assumption is corroborated by the temperature measurements of $\rho(T)$ [8].

Figure 3 demonstrates the temperature dependences of the magnetization of the $\text{V}_{1-x}\text{Mn}_x\text{S}$ samples in the range 4.2–60 K, and Fig. 4 displays the dependences of the magnetization on the magnetic field strength for compositions in the range $0.1 \leq x \leq 0.4$ at a temperature of 4.2 K.

The temperature dependences of the electrical resistivity $\rho(T)$ and the magnetization $\sigma(T)$ for the $\text{V}_{1-x}\text{Mn}_x\text{S}$ sample with $x = 0.2$ in the magnetic field

$H = 2$ kOe in the range 80–300 K are shown in Figs. 5a and 5b, respectively. It can be seen from Fig. 5 that, in the vicinity of T , there is a semimetal–semimetal transition characterized by a weak jump in the resistivity, a hysteresis about 20 K wide, and a dip in the curve of magnetization near T . A small anomaly in the heat capacity C_p is also observed at $T = 157$ K.

As the manganese concentration in the $V_{1-x}Mn_xS$ samples increases up to $x = 0.3$, the metal–dielectric transition is suppressed (Fig. 6).

3. DISCUSSION

3.1. Comparison with the vanadium oxide. The temperature dependences of the resistivity and magnetization in our samples considerably differ from similar dependences for classical compounds of the type VO_2 or V_2O_3 [9, 10]. The $3d$ metal sulfides, as a rule, are characterized by smeared features rather than by abrupt jumps [11]. In this case, the application of the term “metal–dielectric transition” (or “metal–insulator transition”) requires some explanations. In its most restricted sense, this term implies that a metallic state with $dp/dT > 0$ takes place to the one side of the transition point (above T_c in the vanadium oxides) and a dielectric state with the activation type of conductivity is observed to the other side of this point (below T_c in the vanadium oxides). However, it is not unusual that, in the doped systems or in the compounds with bands located in the vicinity of the Fermi level, the transitions are accompanied by small jumps in the resistivity and magnetization as, for example, in the semiconductor–semimetal and metal–semimetal transitions. In this respect, the term “metal–dielectric transition” is applied in a more comprehensive sense to designate any transformations attended by a change in the conductivity type. It is in this sense that the term metal–dielectric transition is used in the present work.

It is quite possible that the observed anomalies are caused by the spitting of the phase diagram for vanadium sulfides due to a high concentration of doping manganese. Even in the absence of manganese, the phase diagram of the nonstoichiometric $V_{1-x}S$ system is very complicated and can be characterized by a large number of superstructures brought about by the ordering of vacancies in the basal planes of the initial NiAs structure [1]. The transitions between these structures are smeared. In the earlier work [7], we found that the doping with iron stabilizes the V_5S_8 superstructure—one of superstructures of the Mn p -type. According to our X-ray diffraction data, a similar structure is observed in the case of manganese doping; however, the question about possible structural distortions upon transitions under discussion remains open. Such distortions, even if they take place, are not large enough to be observed in polycrystalline samples.

3.2. Analysis of the electronic structure of the $V_{1-x}Mn_xS$ system. Since a high-temperature transition

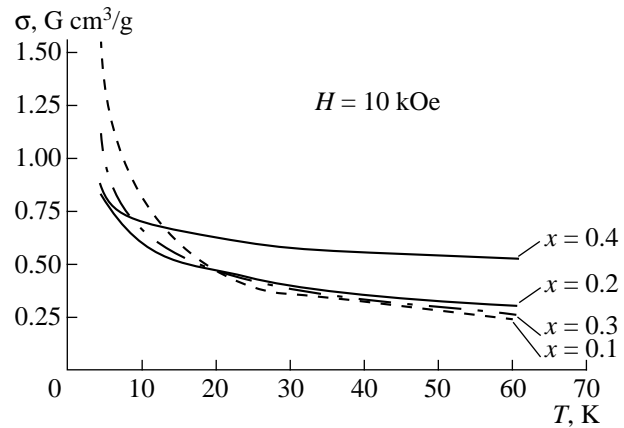


Fig. 3. Temperature dependences of the magnetization of the $V_{1-x}Mn_xS$ samples in the range 4.2–60 K.

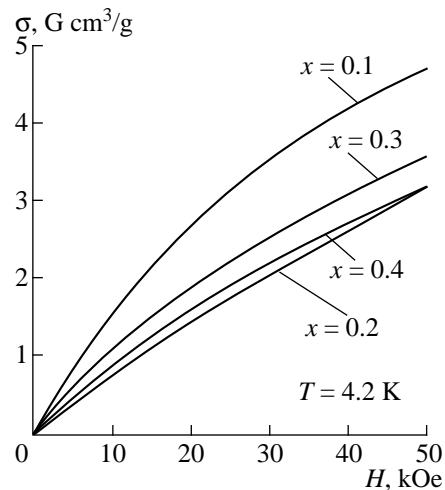


Fig. 4. Dependences of the magnetization on the magnetic field strength for the $V_{1-x}Mn_xS$ samples at 4.2 K.

of the α -VS \rightarrow β -VS type is observed for all the compositions, the α -VS hexagonal phase is taken as the initial phase in our consideration. In this phase, one-electron levels of the V^{2+} (d^3) ion are characterized by the splitting of the cubic t_{2g} triplet into the a_{1g} singlet and the e_u doublet [11]. The band calculations of the VS band structure [12] revealed two almost congruent pockets of the Fermi surface: the electron pocket at the Γ point of the Brillouin zone and the hole pocket near the Brillouin-zone edge at the M point with the nesting vector Q . In the VS band model, the quasi-one-dimensional band a_{1g} is responsible for the nesting, and the e_u band plays the role of an electron reservoir [5]. A change in the electronic structure upon the α -VS \rightarrow β -VS transition is schematically illustrated in Fig. 7. The phase transition, as such, within the model described in [5] is associated with the formation of the exciton dielectric phase (with the generation of the charge density wave in the system of band electrons due to the electron–phonon

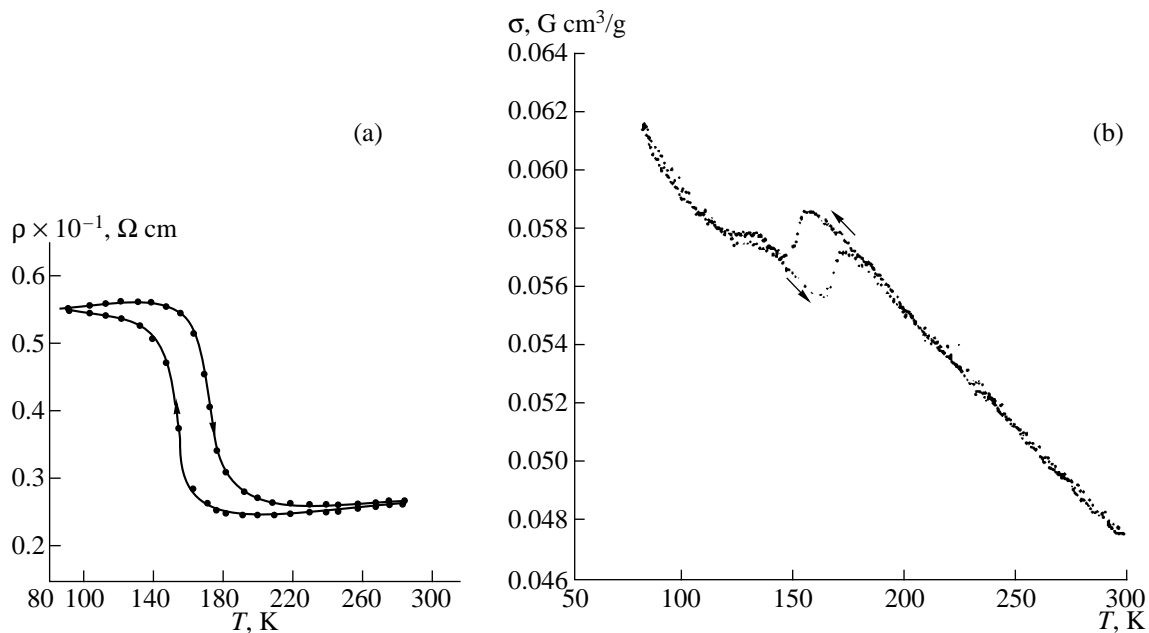


Fig. 5. Temperature dependences of (a) the electrical resistivity and (b) the magnetization of the $V_{1-x}\text{Mn}_x\text{S}$ sample with $x = 0.2$ in a magnetic field of 2 kOe in the range 80–300 K.

coupling). The presence of the e_u band retains the semimetallic properties of the β phase. The effects of electron correlations lead to an increase in the magnetic susceptibility in comparison with the susceptibility of free electrons, but they are not too large to induce the Mott–Hubbard transition.

Our model of changes in the electronic structure upon manganese doping is as follows. Upon replacement of vanadium by manganese, the Mn^{2+} ion adopts the $3d$ configuration. We assume that three t_{2g} electrons

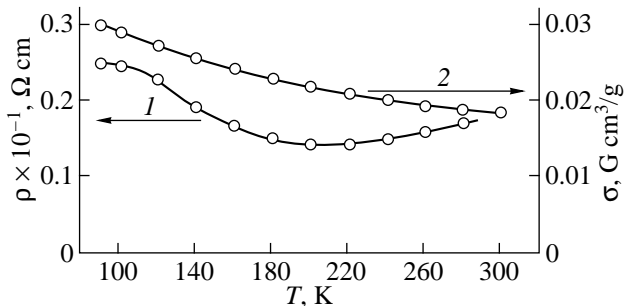


Fig. 6. Temperature dependences of (1) the electrical resistivity and (2) the magnetization of the $V_{1-x}\text{Mn}_x\text{S}$ sample with $x = 0.3$ in a magnetic field of 2 kOe in the range 80–300 K.

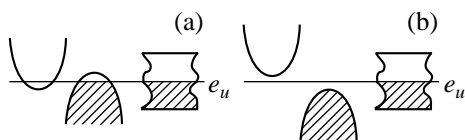


Fig. 7. Schematic representation of the VS electronic structure in (a) α and (b) β phases.

are involved in chemical bonding, like the relevant electrons of the V^{2+} ion, and two e_u electrons give rise to the local magnetic moment $S = 1$ as in the $\text{Fe}_x\text{V}_{1-x}\text{S}$ system [7]. Then, the s – d model of a semimetal with the e_u band with a low density of states at the Fermi level and magnetic impurities with $S = 1$ can serve as an adequate model at small x . The scattering of carries by impurities can lead to the Anderson localization of states in the neighborhood of the Fermi level, which is favored by the low density of states $N(\epsilon_F)$ in the semimetallic e_u band. Hence, the composition with $x = 0.05$ exhibits a semimetallic type of the dependence $\rho(T)$ at low temperatures, whereas the composition with $x = 0.1$ is characterized by a nonmetallic type. At the same time, the Fermi energy ϵ_F lies near the cutoff of mobility ϵ_c , so that $T_A = \Delta\epsilon/K_B = |\epsilon_F - \epsilon_c|/K_B \approx 250$ K (K_B is the Boltzmann constant), and an increase in the temperature brings about the recovery of the semimetallic conductivity. The impurity magnetic moments are localized and provide the Curie–Weiss contribution to the temperature dependences of the magnetic susceptibility and magnetization.

3.3. Discussion of the magnetic properties. In the case of compositions with $x = 0.1$, interactions between magnetic impurities can be ignored; however, at large x values, the effects of interactions become important. The indirect interaction of the Ruderman–Kittel–Kasuya–Yosida (RKKY) type can make both ferrimagnetic and antiferromagnetic contributions; the indirect exchange through anions has an antiferromagnetic nature, so that the situation with competitive exchange interactions seems to be real. The only type of the magnetic order, which can be excluded from the data presented in Fig. 4, is the ferromagnetic interaction. More-

over, the cations in the basal plane of the MnP-type structure form a triangular lattice in which the antiferromagnetic interaction is frustrated even without competition with ferromagnetic interactions [11]. Finally, an increase in the concentration x is accompanied by the delocalization of impurity magnetic moments, and the magnetic properties by themselves should be discussed in terms of the band model. As judged from our data, the latter should be done at $x > 0.3$, when the susceptibility only slightly depends on the temperature and proves to be close to the Pauli susceptibility, while the dependence $\rho(T)$ is rather weak, which is characteristic of semimetals.

As regards the compositions with $x \approx 0.2$, here, apparently, we deal with a complex magnetic behavior caused by the aforementioned reasons. The anomaly in the magnetization near $T = 160$ K is superimposed on the weak Curie–Weiss dependence. It seems likely that the change-over from the localized to band description is characteristic of the given range of compositions; i.e., here, the effects of electron correlations are rather strong. In this case, it is reasonable to expect that changes in the magnetic structure should be accompanied by a jump in the resistivity, as is seen in Fig. 5.

The nature of the magnetic transformation at $T = 160$ K calls for further investigation. A comparison between our data and the results obtained in [1, 2] on doped LaVS_3 permits us to draw the inference that a decrease in the magnetization near T_c in the nonmetallic phase is associated with the singlet states of pairs or clusters. In our case, these states also become possible provided that the frustration is taken into account.

In conclusion, we should note that the mode of localized impurity states at $x = 0.1$ with nonmetallic behavior changes to the band behavior of the system at $x = 0.3$. Intermediate compositions exhibit variations in the electrical and magnetic properties that are characteristic of the metal–dielectric transitions in strongly correlated electronic systems.

ACKNOWLEDGMENTS

We would like to thank É.K. Yakubařlik for his assistance in the performance of magnetic measurements and I.N. Flerov for the low-temperature measurements of heat capacity.

REFERENCES

1. Y. Yasui, T. Nishikawa, Y. Kobayashi, *et al.*, J. Phys. Soc. Jpn. **64**, 3890 (1995).
2. T. Nishikawa, Y. Yasui, Y. Kobayashi, *et al.*, J. Phys. Soc. Jpn. **65**, 2543 (1996).
3. H. Imai, H. Wada, and W. Shiga, J. Phys. Soc. Jpn. **65**, 3460 (1996).
4. T. Nishikawa, J. Takeda, and M. Sato, J. Phys. Soc. Jpn. **63**, 1441 (1994).
5. G. V. Loseva, G. M. Abramova, and S. G. Ovchinnikov, Fiz. Tverd. Tela (Leningrad) **25**, 3165 (1983).
6. A. D. Balaev, Yu. B. Boyarshinov, M. M. Karpenko, *et al.*, Prib. Tekh. Ėksp. **3**, 167 (1985).
7. G. V. Loseva, S. G. Ovchinnikov, T. A. Gařdalova, *et al.*, Fiz. Tverd. Tela (St. Petersburg) **40**, 1890 (1998).
8. N. F. Mott and E. A. Davis, *Electronic Processes in Non-Crystalline Materials* (Oxford Univ. Press, Oxford, 1979; Mir, Moscow, 1982), Vol. 1.
9. N. F. Mott, *The Metal–Insulator Transitions* (Taylor & Francis, London, 1974; Nauka, Moscow, 1979).
10. A. A. Bugaev, B. P. Zakharchenya, and F. A. Chudnovskiř, *The Metal–Semiconductor Phase Transition and Its Applications* (Nauka, Leningrad, 1979).
11. G. V. Loseva, S. G. Ovchinnikov, and G. A. Petrakovskiř, *The Metal–Dielectric Transition in 3rd Metal Sulfides* (Nauka, Novosibirsk, 1983).
12. H. Liu, W. England, and H. Myrol, Solid State Commun. **14**, 1003 (1974).

Translated by O. Borovik-Romanova